(2)

ARMY RESEARCH LABORATORY

Processing and Characterization of Functionally Gradient Ceramic Materials

M. E. O'Day, L. C. Sengupta, E. Ngo,
S. Stowell, and R. Lancto

ARL-TR-337

February 1994

The findings in this report are not to be construed as an official Department of the Army position unless so designated by other authorized documents.

Citation of manufacturer's or trade names does not constitute an official endorsement or approval of the use thereof.

Destroy this report when it is no longer needed. Do not return it to the originator.

REPORT DOCUMENTATION PAGE

Form Approved
OMB No. 0704-0188

1. AGENCY USE ONLY *(Leave blank)*	2. REPORT DATE	3. REPORT TYPE AND DATES COVERED
	February 1994	Final Report

4. TITLE AND SUBTITLE
Processing and Characterization of Functionally Gradient Ceramic Materials

5. FUNDING NUMBERS

6. AUTHOR(S)
M. E. O'Day, L. C. Sengupta, E. Ngo., S. Stowell, and R. Lancto

7. PERFORMING ORGANIZATION NAME(S) AND ADDRESS(ES)
U.S. Army Research Laboratory
Watertown, MA 02172-0001
ATTN: AMSRL-MA-CA

8. PERFORMING ORGANIZATION REPORT NUMBER
ARL-TR-337

9. SPONSORING/MONITORING AGENCY NAME(S) AND ADDRESS(ES)
U.S. Army Research Laboratory
2800 Powder Mill Road
Adelphi, MD 20783-1197

10. SPONSORING/MONITORING AGENCY REPORT NUMBER

11. SUPPLEMENTARY NOTES

12a. DISTRIBUTION/AVAILABILITY STATEMENT
Approved for public release; distribution unlimited.

12b. DISTRIBUTION CODE

13. ABSTRACT *(Maximum 200 words)*

Tape casting of ceramic materials offers the flexibility of gradually altering the electronic or structural properties of two dissimilar systems in order to improve their compatibility. This research outlines the processing and fabrication of two systems of functionally gradient materials. The systems are both electronic ceramic composites consisting of $Ba_{1-x}Sr_xTiO_3$ (BSTO) and alumina or a second oxide additive. These composites would be used in phased array antenna systems, therefore, the electronic properties of the material have specific requirements in the microwave frequency regions. The composition of the tapes are varied to provide a graded dielectric constant, which gradually increases from that of air (dielectric constant = 1) to that of the ceramic (dielectric constant = 1500). This allows maximum penetration of incident microwave radiation as well as minimum energy dissipation and insertion loss into the entire phase shifting device.

14. SUBJECT TERMS
Functionally gradient materials, BSTO, Phase shifting, Tape casting

15. NUMBER OF PAGES
19

16. PRICE CODE

17. SECURITY CLASSIFICATION OF REPORT	18. SECURITY CLASSIFICATION OF THIS PAGE	19. SECURITY CLASSIFICATION OF ABSTRACT	20. LIMITATION OF ABSTRACT
Unclassified	Unclassified	Unclassified	UL

Contents

Figures

Tables

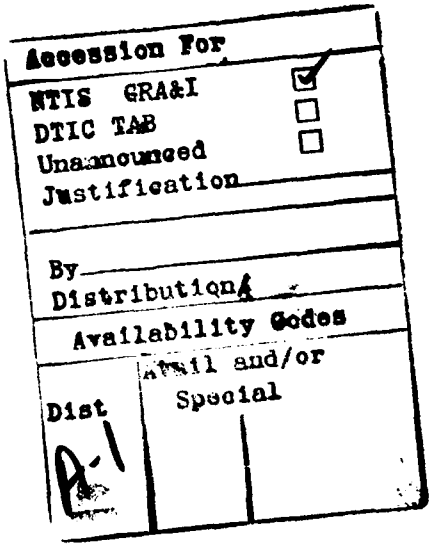

1. INTRODUCTION

Phased array antennas can steer transmitted or received signals either linearly or in two dimensions without mechanically oscillating the antenna. These antennas are currently constructed using ferrite phase shifting elements. Due to the type of circuit requirements necessary to operate these antennas, they are costly, large and heavy. Therefore, the use of these antennas has been limited primarily to military applications and even to those applications which are strategically dependent on such capabilities. If ferroelectric materials could be used instead of ferrites, phased array antennas would be totally revolutionized.

A ceramic Barium Strontium Titanate, $Ba_{.6}Sr_{.4}TiO_3$, (BSTO), electro-optic phase shifter using a planar microstrip construction has been demonstrated.[1] In order to meet the required performance specifications, maximum phase shifting ability, the electronic properties in the low frequency (KHz) and microwave regions (GHz) must be optimized. One obstacle that currently exists is the dielectric mismatch of air (dielectric constant = 1) and BSTO (dielectric constant = 1500). In response to this the concept of functional grading has been applied.

A functionally gradient material (FGM) is a composite material having a microscopically inhomogeneous character. It was first proposed in 1984 motivated by the need for a material that would withstand the severe service conditions of a space plane. In that instance a thermal barrier coating that would join a metal to a ceramic was of interest. This concept can easily be applied to any two systems with dissimilar properties. In the case of BSTO and air a grading of the dielectric constant would allow maximum penetration of incident microwave radiation as well as minimum energy dissipation and insertion loss into the entire phase shifting device.

Tape casting is a low-cost process for making high-quality laminated materials for which an adequate thickness control and good surface finish are required.[2-5] It is a process directly related to slip casting that consists of preparing a stable slip of a ceramic powder in an aqueous or nonaqueous liquid. It is currently used for fabrication of a variety of ceramic substrates and multilayer capacitors. Tape casting is especially well suited to preparing wide, flat, uniform ceramic tapes with smooth surfaces, precise dimensional tolerances and adequate green strength for handling. In the area of producing a functionally gradient composite this technique offers the flexibility of gradually altering the electronic properties of each layer to produce a gradual and continuous grading of the dielectric constant.

The matching layers are comprised of a ferroelectric, BSTO ($Ba_{.6}Sr_{.4}TiO_3$) and a non-ferroelectric, low dielectric, low loss ceramic such as alumina. The BSTO-Alumina composite has a patent pending on its formulations and the other composite which is designated herein as BSTO-Oxide II currently has a patent undergoing the filing process. The composites that correspond to the formulations of the individual matching layers have been developed independently as beam steering (phase shifting) materials for antennas where a reduced dielectric constant and loss tangent are necessary. Therefore, the materials chosen for producing these functionally graded materials can be used as beam steering materials themselves depending on the electronic properties required in a particular antenna application.

2. EXPERIMENTAL

2.1 Ceramic Processing

Powdered forms of Barium Titanate and Strontium Titanate were obtained from Ferro Corporation, Transelco Division, Pen Yan, N.Y. (product nos. 219-6 and 218 respectively) and stoichiometrically mixed to achieve $Ba_{.6}Sr_{.4}TiO_3$. The resulting BSTO was mixed with either powder Alumina (ALCOA Industrial Chemicals, Bauxite, AR, distributed by Whittaker, Clark, and Daniels, South Plainfield, N.J., product no. A16-SG) or a second oxide (Oxide II) in the proper weight percent.

Layers for use in a laminated graded stack were then processed via aqueous based tape casting. For each layer the proper BSTO/oxide mixture was combined into an aqueous based slurry using the formula listed in Table I. Following slurry preparation tapes were cast onto Plexiglass using an 8" doctor blade (Paul Gardener Co., Pompano Beach, FA) at a thickness calculated based on the following equation:

$\varepsilon' = Ct/A\varepsilon_0$ where (1)

ε' = dielectric constant of the layer
C = capacitance of BSTO
t = thickness
A = area
$\varepsilon_0 = 8.8542 \times 10^{-12}$ F/m

The schematics of the layer formulations and layer thicknesses for the two types of composite graded laminate stacks are shown in Fig. 1. As shown in these figures a constant capacitance was maintained by adjusting the layer thickness which insures a linear voltages profile across the tape layers, e.g., layers for Al_2O_3 are much thinner than BSTO layers. After casting tapes were placed in a humidity drying oven (Tabal Palatinous Rainbow P-3G) at 95% relative humidity and 35°C for approximately 36 hours. The tapes peeled easily from the Plexiglass once they were dry and were punched into 3/4" circles for pressing. The tapes were stacked and placed in a steel die which was subsequently heated to around 200°C before pressing. Sintering was then done in a CM box furnace without any applied pressure.

Bulk samples corresponding to layer compositions were processed by adding Rhoplex B-60A (Rohm and Haas Co., Philadelphia, PA) which is a 3wt% organic binder consisting of an aqueous emulsion of acrylic polymer to the BSTO/oxide mixture. Each sample is then air-dried and pressed to approximately 7,000 psi., and sintered following a schedule that was ascertained by employing a deflectometer such as a Mitutoyo digimatic indicator and miniprocessor (Mitutoyo Corp., Paramus, N.J.). The densities, % Porosity and % Absorption are given in Table II. It should be noted that all of the examined samples have % liquid absorption of less than 2%.

TABLE I. Aqueous Based Slip Formulation.

BSTO/oxide mixture	46.00	g
Darvan C	0.12	g
Distilled H_2O (Room Temp.)	27.50	g
glycerin	1.50	g
P-1200*	.50	g
Methocel (20-214)+	2.00	g
Distilled H_2O (90°C)	20.00	g
Distilled H_2O (Room Temp.)	23.50	g

2.2 Metallization

Metallization was accomplished by painting on two circular, aligned electrodes on either side of the specimens using high purity silver paint made by SPI Supplies West Chester, PA. Wires were then attached using high purity silver epoxy, Magnobond 8000, made by Magnolia Plastics, Inc., Chamblee, GA.

2.3 Electronic Measurements

The dielectric constants, ε', loss tan δ, % tunability were determined for all tape stacks and bulk samples corresponding to layer compositions. The dielectric constant, ε', where

$\varepsilon = \varepsilon' + i\varepsilon''$ (2)

is a complex function. The loss tan δ can be defined as:

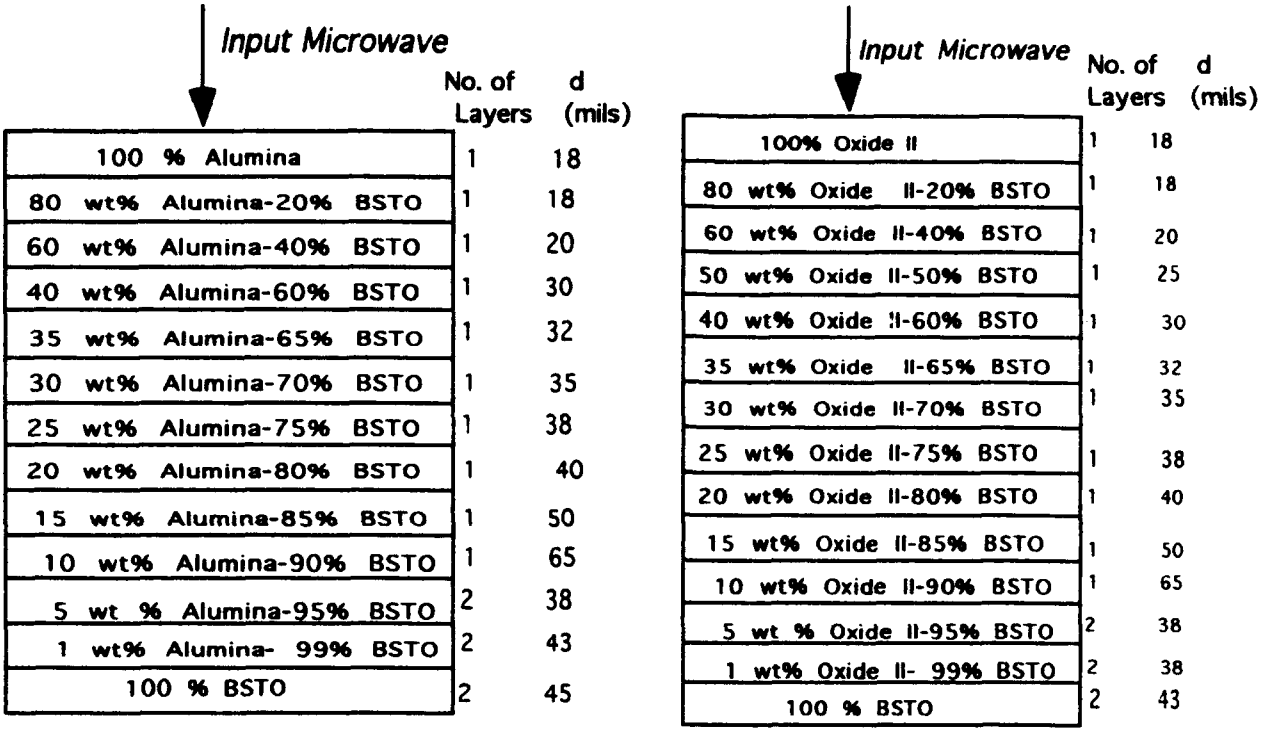

Fig. 1. Schematics of the layer formulations and thicknesses for two types of composite graded laminate stacks.

$$\tan \delta = \varepsilon'' / \varepsilon' \tag{3}$$

$$\% \text{ tunability} = \{ \varepsilon'(0) - \varepsilon'(Vapp)\}/ \{\varepsilon'(0)\} \tag{4}$$

The tunability measurements were taken with an applied electric field which ranged from 0 to 3.0 V/micron (μm). The electronic properties given in the tables were measured at a frequency of 1 KHz. Capacitance measurements for all materials were taken using an HP4284A LCR meter and the dielectric constants were calculated using equation (1) and the sample dimensions. The dielectric constant has been calculated from the corrected capacitance values, C_{corr}, according to equation (5)[6]. The edge (fringe) capacitance, C_e, was calculated from either equation (6) or (7) depending on electroding configuration. These equations assume that the ground capacitance is zero and the thickness of the metal layer is much less than the thickness of the specimen.

$$C_{corr} = C_{meas} - C_e \text{ where } C_{meas} = \text{measured capacitance value and } C_e \text{ is defined below} \tag{5}$$

Equal electrodes smaller than the specimen:

$$C_e = (0.0019\, C_{meas} - 0.00252 \ln t + 0.0068)\, P \tag{6}$$

Diameter of the electrodes = diameter of the specimen:

$$C_e = (0.0041\, C_{meas} - 0.0034 \ln t + 0.0122)\, P \tag{7}$$

where $P = \pi (d_{electrode} + t)$ and $d_{electrode}$ = diameter of the electrode and t = thickness of the specimen.

TABLE II. Sample Descriptions Tape Stacks and Bulk Samples Corresponding to Layer Compositions.

BSTO-Alumina

Sample	*Density (g/cc)*	*% Porosity*	*% Absorption*
STACK #1 (BSTO-20% Alumina -BSTO)	4.391	25.68	5.03
STACK #2 (BSTO-60% Alumina BSTO)	warped	30.11	6.91
STACK#3 (BSTO-100% Alumina)	warped	32.10	8.51
Bulk Ceramics Corresponding to Layer Compositions			
0 wt% Al_2O_3	5.373	3.16	0.48
1 wt% Al_2O_3	5.319	8.94	1.43
5 wt% Al_2O_3	4.744	6.63	1.10
10 wt% Al_2O_3	4.687	7.15	1.22
20 wt% Al_2O_3	4.222	7.81	1.46
30 wt% Al_2O_3	3.965	5.05	1.03
60 wt% Al_2O_3	3.797	5.47	1.20
80 wt% Al_2O_3	3.615	7.48	1.72
pure Al_2O_3	3.992	4.44	0.95

BSTO-Oxide II

Sample	*Density (g/cc)*	*% Porosity*	*% Absorption*
STACK (BSTO-100% Oxide II)	5.07	2.63	1.37
Bulk Ceramics Corresponding to Layer Compositions			
1 wt% Oxide II	5.22	10.31	1.64
5 wt% Oxide II	5.28	8.86	1.51
10 wt% Oxide II	5.30	7.67	1.23
15 wt% Oxide II	5.12	8.27	1.28
20 wt% Oxide II	5.37	10.31	1.64
25 wt% Oxide II	5.44	14.24	2.33
30 wt% Oxide II	5.40	9.73	1.60
40 wt% Oxide II	5.36	10.59	1.67
50 wt% Oxide II	5.22	10.34	1.70
60 wt% Oxide II	5.38	10.28	1.58

3. RESULTS AND DISCUSSION

3.1 SEM and EDX Analysis

The SEM micrograph of a representative BSTO-Alumina laminate stack displayed in Fig. 2(a) reveals that although the stack is comprised of several individual layers, it appears structurally continuous throughout the cross-section. SEM examination of the individual bulk ceramic layers of the BSTO-Alumina composite revealed that a second phase became apparent in alumina additions as low as 10 wt% becoming more dominant at 35 wt% alumina and then disappearing by the time 60 wt% is achieved. Micrographs for these microstructures are displayed in Figs. 2(b) - 2(d). EDX of the small grains revealed a depletion in alumina while EDX of the larger, smoother grains displayed an increase in the alumina content. This suggests the formation of a barium aluminum titanium oxide phase.

A photograph of the stack and of its cross-section are presented in Figs. 2(a) and 2(b). The laminated and sintered stack of BSTO-Oxide II maintained a much higher integrity than it's BSTO-Alumina counterpart. This has been attributed to the similar densities and sintering temperatures of these two materials. SEM examination of the individual BSTO-Oxide II compositions showed very little microstructural difference with added percentages of oxide. A small reduction in grain size was the most apparent difference. A micrograph of a typical BSTO-Oxide II microstructure is shown in Fig. 2(c). EDX analysis of the individual layers showed no unusual behavior with the percentage of zirconium gradually increasing with steady decreases in barium, strontium and titanium.

3.2 X-Ray Diffraction

A summary of the X-Ray diffraction results for the various compositions of the BSTO composites are given in Table III. In agreement with EDX, the results reveal that when alumina is added to BSTO in small amounts, < 20%, a second phase of Barium Aluminum Titanate, $Ba_3Al_{10}TiO_{20}$, is formed in compositions having between 20 and 40% alumina another second phase of Barium Aluminum Titanate forms ie. $BaAl_6TiO_{12}$. In this composition range, we are also seeing traces of Barium Aluminum Oxide. By the time the composition reaches 60% alumina no forms of Barium Aluminum Titanate are detectable. Only faint traces of BSTO are discernible at this composition. It should be noted that there are three forms of Barium Aluminum Oxide as follows 1) $BaAl_{12}O_{19}$ 2) $BaAl_{9.2}O_{14.8}$ and 3) $BaAl_{13.2}O_{20.8}$ and that at 60% alumina we were unable to discern which phase was most prevalent or even if all three phases were present. At 80% alumina a specific phase of Barium Aluminum Oxide still cannot be identified, but definite Al_2O_3 peaks became apparent. Pure alumina provided a complete diffraction pattern.

The results for the BSTO-Oxide II composites reveal a completely different picture. By looking at the results given in Table III we immediately observe that initial Oxide II appears to be absorbed into the BSTO lattice structure. At compositions from 5% - 50 % Oxide II, BSTO is the more dominant pattern, but at 60%, Oxide II becomes predominant. It is also interesting to note that no second phase materials were detected at any of the compositions for this composite.

3.3 Electronic Properties

The results for the electronic properties of the BSTO-Alumina laminated stacks and the BSTO-Alumina composites corresponding to laminate layer compositions are shown in Table IV. Three separate stack compositions were fabricated as shown. Stack #1 includes pure BSTO to 20 wt% Alumina-BSTO composite layer, stack #2 is comprised of BSTO to 60 wt% alumina and stack #3 consists of BSTO to 100% alumina. As seen in the table all of the specimens (laminates and bulk) have low loss and are readily tunable. In the bulk specimens the dielectric constant of the samples are quickly reduced up to 35 wt% alumina at which point the rate of reduction in the dielectric constant is diminished. The dielectric loss, tan δ, reported here includes the loss caused by the metal contact. Improved metallization for these materials will definitely result in tan $\delta < 0.01$. The tunability of the specimens could be increased with an increase in applied field by using thinner specimens. Even so, the tunability of the composites is maintained at reasonable levels (>10%) up to 20 wt% alumina at which time the tunability decreases rapidly. A graph of the tunability versus applied field is shown in Fig. 4. The inset shows the dielectric constant of these compositions versus tunability at an electric field of 0.7 V/μm. The semi-log plot of the dielectric

2(a)

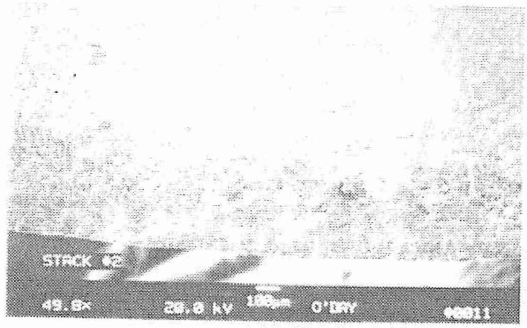

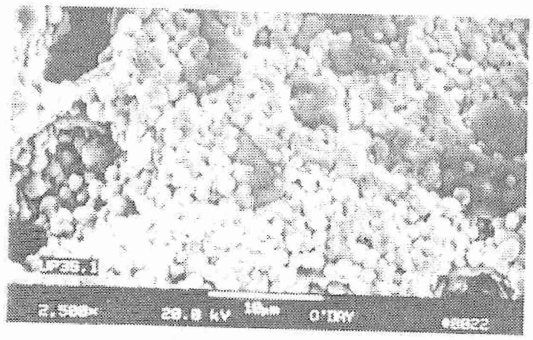

2(b)

2(c)

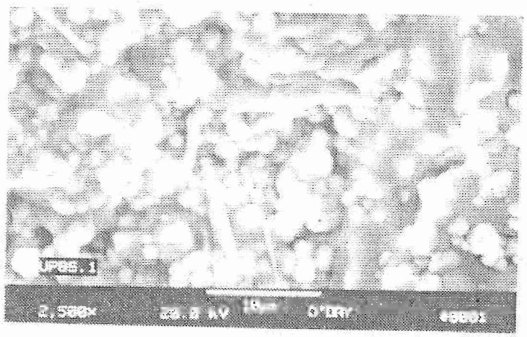

2(d)

Fig. 2. SEM micrographs of (a) BSTO-Alumina laminated tape stack, (b) BSTO-10wt% Alumina bulk ceramic composite, (c) BSTO-35 wt% Alumina bulk ceramic composite, and (d) BSTO-60 wt% Alumina bulk ceramic composite microstructures.

3(a)

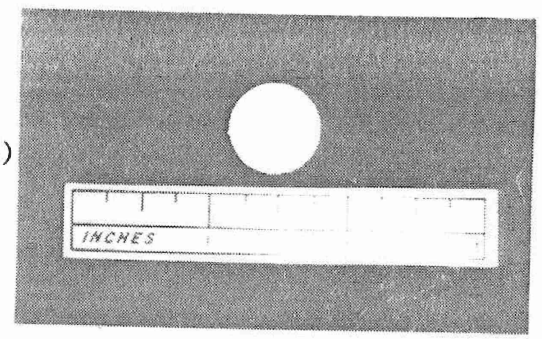

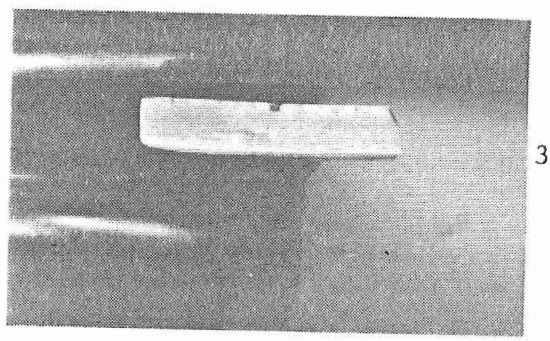

3(a)

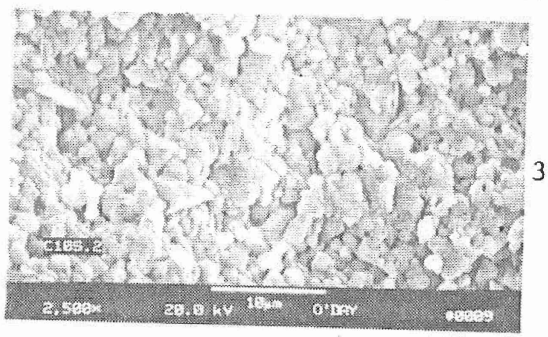

3(b)

Fig. 3. (a) Optical micrograph of BSTO-Oxide II laminated tape stack (side and top view) (b) SEM micrograph of BSTO-40 wt% Oxide II bulk ceramic composite microstructure.

TABLE III. X-Ray Diffraction Results.

BSTO-Alumina

Bulk Ceramics Corresponding to Layer Compositions	*Detected Phases*
pure BSTO	Full pattern for $Ba_{.6}Sr_{.4}TiO_3$
1 wt% Al_2O_3	BSTO and $Ba_3Al_{10}TiO_{20}$
5 wt% Al_2O_3	BSTO and $Ba_3Al_{10}TiO_{20}$
10 wt% Al_2O_3	BSTO and $Ba_3Al_{10}TiO_{20}$
15 wt% Al_2O_3	BSTO and $Ba_3Al_{10}TiO_{20}$
20 wt% Al_2O_3	BSTO, $Ba_3Al_{10}TiO_{20}$ and $BaAl_{13.2}O_{20.8}$
25 wt% Al_2O_3	BSTO, $Ba_3Al_{10}TiO_{20}$, $BaAl_6TiO_{12}$ and $BaAl_{13.2}O_{20.8}$
30 wt% Al_2O_3	$Ba_3Al_{10}TiO_{20}$, $BaAl_6TiO_{12}$, BSTO and $BaAl_{13.2}O_{20.8}$
35 wt% Al_2O_3	$Ba_3Al_{10}TiO_{20}$, $BaAl_6TiO_{12}$, BSTO and $BaAl_{13.2}O_{20.8}$
40 wt% Al_2O_3	$Ba_3Al_{10}TiO_{20}$, $BaAl_6TiO_{12}$, BSTO and $BaAl_{13.2}O_{20.8}$
60 wt% Al_2O_3	Barium Aluminum Oxide - phase unknown and BSTO
80 wt% Al_2O_3	Barium Aluminum Oxide - phase unknown and Al_2O_3
pure Al_2O_3	Full Al_2O_3 pattern

BSTO-Oxide II

Bulk Ceramics Corresponding to Layer Compositions	*Detected Phases*
1 wt% Oxide II	BSTO
5 wt% Oxide II	BSTO and Oxide II
10 wt% Oxide II	BSTO and Oxide II
15 wt% Oxide II	BSTO and Oxide II
20 wt% Oxide II	BSTO and Oxide II
25 wt% Oxide II	BSTO and Oxide II
30 wt% Oxide II	BSTO and Oxide II
35 wt% Oxide II	BSTO and Oxide II
40 wt% Oxide II	BSTO and Oxide II
50 wt% Oxide II	BSTO and Oxide II
60 wt% Oxide II	Oxide II and BSTO
80 wt% Oxide II	Oxide II and BSTO
pure Oxide II	Full Oxide II pattern

constant for both the BSTO-Alumina composites and the BSTO-Oxide II composites is shown in Fig. 5. As shown in Fig. 5, a change in the slope occurs at a composition of 20–40 wt% alumina, which may correspond to the formation of the additional second phase $BaAl_6TiO_{12}$. The dielectric constant of the laminated tape stack of the BSTO composite layers can be calculated by assuming a series capacitance between the layers and a uniform shrinkage rate for all layers. In this case the dielectric constant is represented by equation (8):

$$1/\varepsilon_{stack} = 1/t_{stack} \{[(t \text{ layer } \#1) / (\varepsilon \text{layer } \#1)] + \ldots\ldots + [(t \text{ layer } n) / (\varepsilon \text{layer } n)]\} \quad (8)$$

The calculated value for the dielectric constant of the BSTO-Alumina laminated stack #1 was 921.83 as compared to the measured value found in Table IV which was 657. For stack #2, the calculated value was 129.10 relative to the

TABLE IV. Electronic Properties of BSTO (Ba = .6) and Alumina Laminated Tape Stacks and Corresponding Bulk Ceramic Compositions.

Sample	*Dielectric Constant*	*Loss Tangent*	*% Tunability*	*Electric Field (V/μm)*
STACK #1 (BSTO-20wt% Alumina)	657.00	0.0236	13.00	0.70
STACK #2 (BSTO-60 wt% Alumina)	121.88	0.0202	0.35	0.70
STACK #3 (BSTO-100% Alumina)	93.91	0.0210	0.65	0.70
Bulk Ceramics Corresponding to Layer Compositions				
Alumina Content (wt %)				
1.0	2606.97	0.0122		
5.0	1260.53	0.0630*	13.88	0.67
10.0	426.74	0.0163	4.79	0.39
15.0	269.25	0.0145		
20.0	186.01	0.0181	3.58	0.48
25.0	83.07	0.0120		
30.0	53.43	0.0135	5.13	2.21
35.0	27.74	0.0029		
40.0	25.62	0.1616*		
60.0	16.58	0.0009	0.01	0.60
80.0	12.70	0.0016		
100.0	8.37	0.0036		

* samples had poor contacts

measured of 121.88. Stack #3 had a calculated value of 105 as compared to a measured value of 93.11. The reason for any discrepancies could be due differences in densities between the tape and bulk materials. Also, the area of the tapes did shrink uniformly. Therefore, the assumption that the area of the stack was the same as each individual tape is not entirely correct. As indicated previously, second phases consisting of various stoichiometries BaAlTiO ($Ba_3Al_{10}TiO_{20}$, $BaAl_6TiO_{12}$ and $BaAl_{13.2}O_{20.8}$) are formed in the bulk ceramics. It is not clear at this time if the same formations will occur in tape specimens. The reason that the calculated dielectric constant of stack #1 was much less than the measured value (28% difference) relative to 5% difference for stack#2 and 11% difference for stack#3 can be seen by examining equation (8). For stack #1, the variation in the thickness and the dielectric constant of the layers has bigger effect on the overall dielectric constant of the laminated stack. Therefore, non-uniformity in thicknesses and differences in dielectric constants between bulk ceramic and tape specimens will have a much greater effect on stack #1. The tunability of stack #1 was 13.00% at an applied field of 0.7 V/μm. If the dielectric constant for stack #1 is taken from the graph contained in Fig. 4 (inset), then the value expected for that tunability would be between 10-13%. The tunabilities of stack #2 and stack #3 are too small to make this comparison (too small to read accurately from the inset in Fig. 4). In general the accuracy associated with finding the tunability from Fig 4. (inset) is not very good. However, differences between these bulk ceramic and tape tunabilities (assuming identical dielectric constants) would be due to the fact the electric across the layered materials is not uniform as in the case of the bulk ceramic with equivalent dielectric constant.

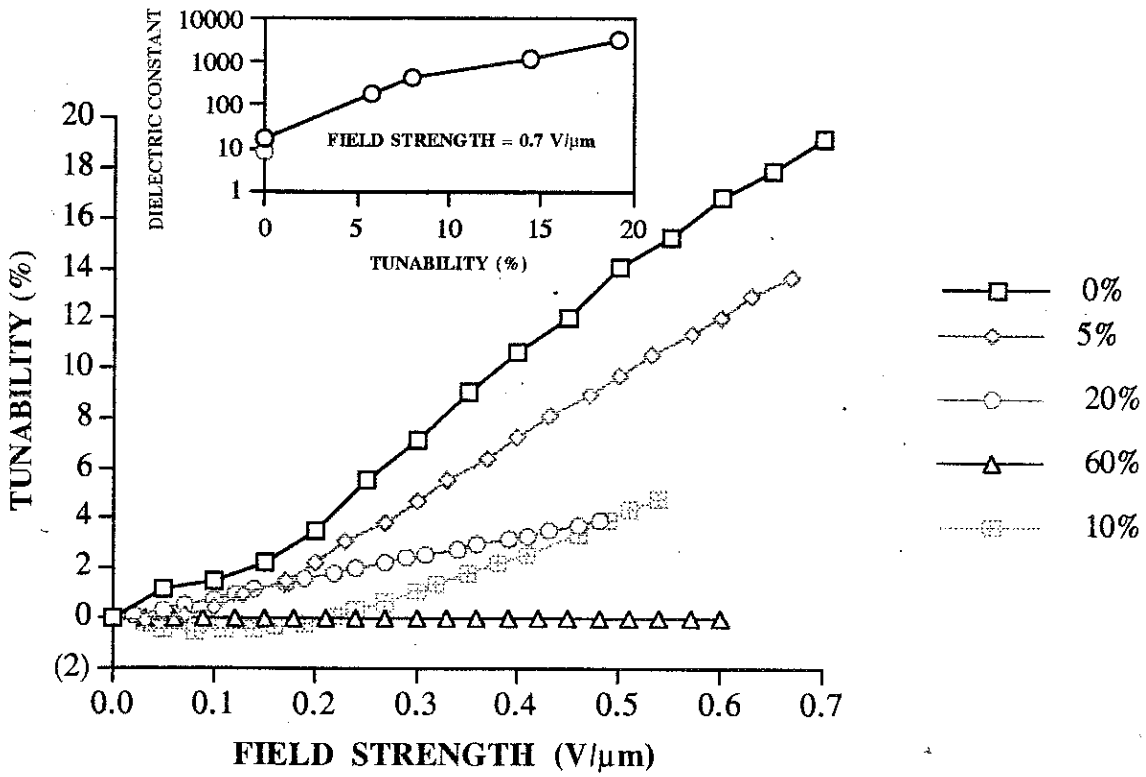

Fig. 4. Tunability (%) versus Applied Electric Field (V/μm) for BSTO-Alumina composites (inset shows the Dielectric Constant versus Tunability (%) at an electric field of 0.7 V/μm).

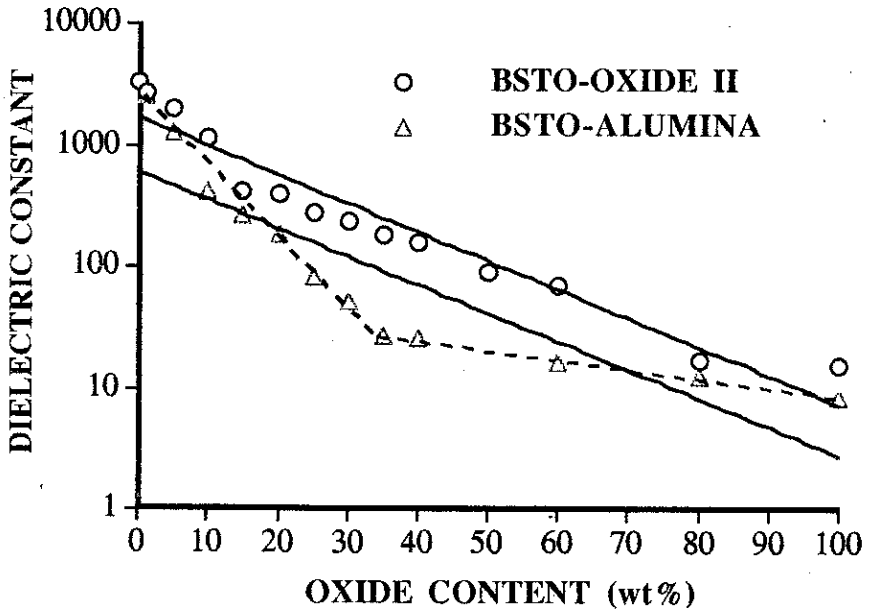

Fig. 5. Semi-log plot of the Dielectric Constant versus Alumina and Oxide II Content for BSTO-Alumina and BSTO-Oxide II composites.

Table V contains the electronic data for the BSTO-Oxide II laminated stack and the bulk ceramics corresponding to the individual layer compositions. As shown in Table V the loss tangent of the materials are relatively low (<0.02). It appears that as the dielectric constant decreased the loss decreased. The dielectric constant of the composites decreases with the addition of Oxide II content. As shown in Fig. 5, the rate of reduction is similar to that of BSTO-Alumina composites for compositions < 20%. However, between 20 wt% - 50 wt% the rate of reduction in the dielectric constant is less than that of the BSTO-Alumina composites. The decrease in the dielectric constant for the two sets of composites is again similar from 60 wt% - 100 wt% additive content. However, the magnitude of the dielectric constant for all of the BSTO-Alumina composites is less than that of the BSTO-Oxide II composites. This may be due to the formation of the second phases in the BSTO-Alumina composites.

TABLE V. Electronic Properties of BSTO (Ba = .6) and Oxide II Laminated Tape Stacks and Corresponding Bulk Ceramic Compositions.

Sample	*Dielectric Constant*	*Loss Tangent*	*% Tunability*	*Electric Field (V/mm)*
STACK (BSTO-100% Oxide II)	198.03	0.0132	2.06	0.70
Oxide II Content (wt %)				
0.0	3299.08	0.0195	19.91	0.73
1.0	2696.77	0.0042	46.01	2.72
5.0	2047.00	0.0138	12.70	0.76
10.0	1166.93	0.0111	7.68	0.68
15.0	413.05	0.0159		
20.0	399.39	0.0152	5.39	0.76
25.0	273.96	0.0240	6.02	1.02
30.0	233.47	0.0098		
35.0	183.33	0.0091	5.87	0.95
40.0	162.26	0.0095		
50.0	92.73	0.0071	1.67	1.12
60.0	69.80	0.0098		
80.0	17.31	0.0056		
100.0	15.98	0.0018	0.05	0.27

The Tunability (%) versus Applied Electric Field for several compositions of BSTO-Oxide II composites is shown in Fig. 6. The inset represents the Dielectric Constant of these compositions versus Tunability (%) at an electric field of 0.7 V/um. It is apparent that the tunability decreases for compositions less than 30 wt% Oxide II. For additive contents >25 wt% and at similar electric fields, the tunability of the BSTO-Oxide II composites is greater than that of the BSTO-Alumina composites. This may again be due to the formation of second phases in the BSTO-Alumina composites, creating additional non-ferroelectric phases which inhibit tuning in the material. The calculated value for the dielectric constant of the BSTO-Oxide II laminated tape stack using equation (8) was 193.00 as compared to the measured value of 198.03 (average of several measured identical tape stacks). This represents a percent difference of 2.6%. The excellent agreement between the measured and calculated values seems to indicate a lack of diffusion between the layers. The percent difference in these composite laminates was less than the BSTO-Alumina laminates because the area of these tapes was indeed the same as the stack (the shrinkage rate of the layers was consistent) and the material does not form any second phases. Non-uniformity in tape thickness is still present and was observed when the dielectric constants of several identical stacks were measured and were seen to vary. If the dielectric constant of the stack is taken from the inset in Fig. 6 then the expected value for the tunability would be around 2.00% relative to the measured value of 2.06%.

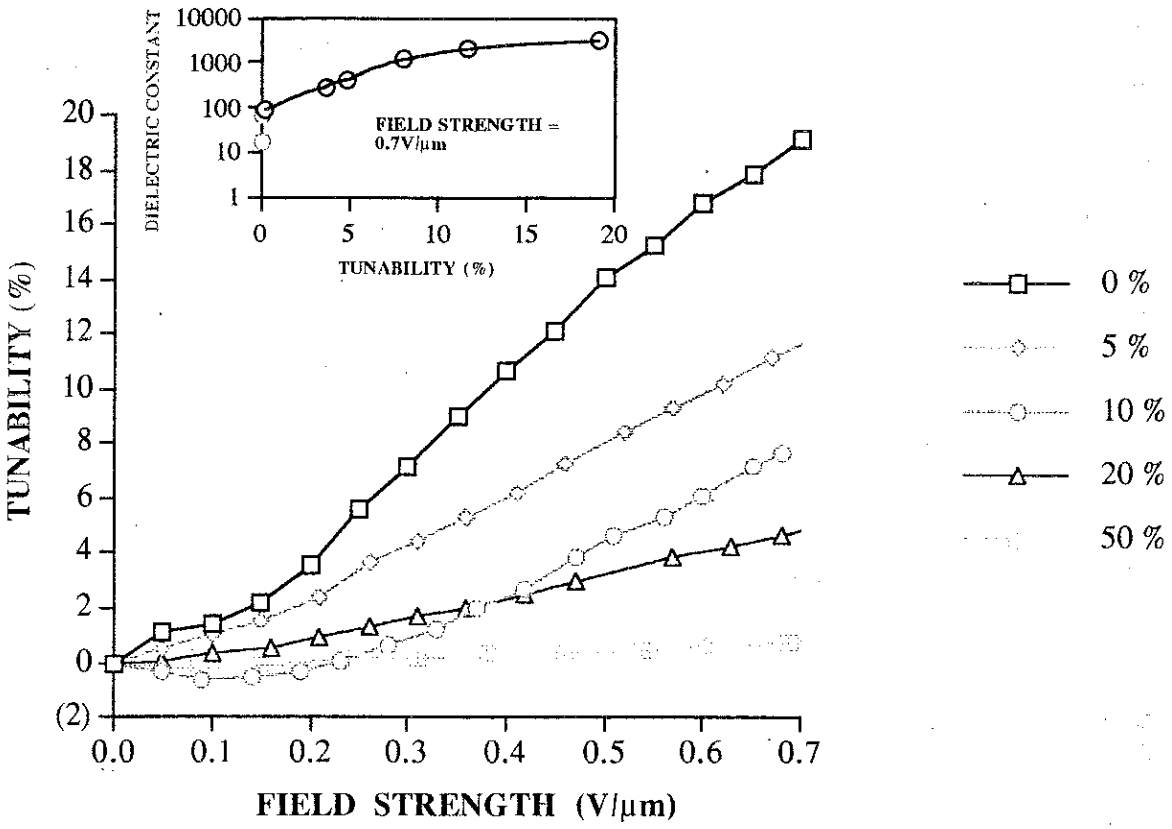

Fig. 6.Tunability (%) versus Applied Electric Field (V/μm) for BSTO-Oxide II Composites (inset shows the Dielectric Constant versus Tunability (%) at an electric field of 0.7 V/μm).

4. CONCLUSIONS

In conclusion, we have demonstrated the possibility of grading the dielectric constant of BSTO-ceramic composites to produce matching layers for use in phased array antennas. It has been shown to be successful using two types of BSTO ceramic composites. These composites were chosen due to their adjustable dielectric constants, low loss and high tunability. Using these materials is superior to using non-ferroelectric layers such as magnesium strontium zirconium titanate or any other matching schemes. These graded layers also provide a smooth built-in matching scheme which eliminates the possibility of air gaps between the layers and the beam steering portion of the device (BSTO). The electronic properties of the laminates showed that the compositions of the layers were maintained upon firing (minimal diffusion occurred).

The BSTO-Alumina laminate was more difficult to fabricate and was found to warp and crack upon sintering due to the large difference in densities between BSTO and alumina. The other composite laminated stack did not warp or crack due to the very similar densities of BSTO and Oxide II. The BSTO-Alumina composites were seen to form second phases which begin to inhibit tunability after 25 wt% Alumina. The dielectric constant of these composites decreases faster so a smaller number of matching layers is necessary. If the composites are used as beam steering sections an antenna with a lower dielectric constant requirement may be constructed. The BSTO-Oxide II composites have higher dielectric constants and higher tunabilities and can be used in applications where these properties are applicable.

5. ACKNOWLEDGMENTS

- The authors would like to thank Phillip Wong, ARL-MD, for his contributions to the SEM and EDX work in this paper. Also, the assistance of Daniel Snoha and Kyu Cho, ARL-MD, with the "all" of the X-ray diffraction data is greatly appreciated.

6. REFERENCES

1. R.W. Babbitt, T.E. Koscica, and W.E. Drach, "Planar Microwave Electro-optic Phase Shifters," *Microwave Journal*, **35** [6] 63-79 (1992).

2. D.J. Shanefield and R.E. Mistler, "Fine-Grained Alumina Substrates: I. The Manufacturing Process," *Am. Ceram. Soc. Bull.*, **53** [5] 416-20 (1974).

3. D.J. Shanefield, P.T. Morzenti, and R.E. Mistler, "Fine-Grained Alumina Substrates: II. Properties," *Am. Ceram. Soc. Bull.*, **53** [8] 564-68 (1974).

4. R.E. Mistler, D.J. Shanefield, and R.B. Runk, "Tape Casting of Ceramics," pp. 411-88 in Ceramic Processing Before Firing. Edited by G.Y. Onoda and L.L. Hench. Wiley, New York, 1978.

5. R. Moreno, "The Role of Slip Additives in Tape-Casting Technology: Part I-Solvents and Dispersants," *Am. Ceram. Soc. Bull.*, **71** [10] 1521-31 (1992).

6. A.H. Scott and H.L. Curtis, "Edge Correction in the Determination of Dielectric Constant," *J. of Res.*, UNBAA, Nat. Bureau of Standards, 22, 747-75 (1939).

DISTRIBUTION LIST

No. of Copies	To
1	Office of the Under Secretary of Defense for Research and Engineering, The Pentagon, Washington, DC 20301
	Director, U.S. Army Research Laboratory, 2800 Powder Mill Road, Adelphi, MD 20783-1197
1	ATTN: AMSRL-OP-SD-TP, Technical Publishing Branch
1	AMSRL-OP-SD-TM, Records Management Administrator
	Commander, Defense Technical Information Center, Cameron Station, Building 5, 5010 Duke Street, Alexandria, VA 23304-6145
2	ATTN: DTIC-FDAC
1	MIA/CINDAS, Purdue University, 2595 Yeager Road, West Lafayette, IN 47905
	Commander, Army Research Office, P.O. Box 12211, Research Triangle Park, NC 27709-2211
1	ATTN: Information Processing Office
	Commander, U.S. Army Materiel Command, 5001 Eisenhower Avenue, Alexandria, VA 22333
1	ATTN: AMCSCI
	Commander, U.S. Army Materiel Systems Analysis Activity, Aberdeen Proving Ground, MD 21005
1	ATTN: AMXSY-MP, H. Cohen
	Commander, U.S. Army Missile Command, Redstone Arsenal, AL 35809
1	ATTN: AMSMI-RD-CS-R/Doc
	Commander, U.S. Army Armament, Munitions and Chemical Command, Dover, NJ 07801
2	ATTN: Technical Library
	Commander, U.S. Army Natick Research, Development and Engineering Center, Natick, MA 01760-5010
1	ATTN: Technical Library
	Commander, U.S. Army Satellite Communications Agency, Fort Monmouth, NJ 07703
1	ATTN: Technical Document Center
	Commander, U.S. Army Tank-Automotive Command, Warren, MI 48397-5000
1	ATTN: AMSTA-ZSK
1	AMSTA-TSL, Technical Library
	Commander, White Sands Missile Range, NM 88002
1	ATTN: STEWS-WS-VT
	President, Airborne, Electronics and Special Warfare Board, Fort Bragg, NC 28307
1	ATTN: Library
	Director, U.S. Army Research Laboratory, Weapons Technology, Aberdeen Proving Ground, MD 21005-5066
1	ATTN: AMSRL-WT

No. of Copies	To
	Commander, Dugway Proving Ground, UT 84022
1	ATTN: Technical Library, Technical Information Division
	Commander, U.S. Army Research Laboratory, 2800 Powder Mill Road, Adelphi, MD 20783
1	ATTN: AMSRL-SS
	Director, Benet Weapons Laboratory, LCWSL, USA AMCCOM, Watervliet, NY 12189
1	ATTN: AMSMC-LCB-TL
1	AMSMC-LCB-R
1	AMSMC-LCB-RM
1	AMSMC-LCB-RP
	Commander, U.S. Army Foreign Science and Technology Center, 220 7th Street, N.E., Charlottesville, VA 22901-5396
3	ATTN: AIFRTC, Applied Technologies Branch, Gerald Schlesinger
	Commander, U.S. Army Aeromedical Research Unit, P.O. Box 577, Fort Rucker, AL 36360
1	ATTN: Technical Library
	U.S. Army Aviation Training Library, Fort Rucker, AL 36360
1	ATTN: Building 5906-5907
	Commander, U.S. Army Agency for Aviation Safety, Fort Rucker, AL 36362
1	ATTN: Technical Library
	Commander, Clarke Engineer School Library, 3202 Nebraska Ave., N, Fort Leonard Wood, MO 65473-5000
1	ATTN: Library
	Commander, U.S. Army Engineer Waterways Experiment Station, P.O. Box 631, Vicksburg, MS 39180
1	ATTN: Research Center Library
	Commandant, U.S. Army Quartermaster School, Fort Lee, VA 23801
1	ATTN: Quartermaster School Library
	Naval Research Laboratory, Washington, DC 20375
2	ATTN: Dr. G. R. Yoder - Code 6384
	Chief of Naval Research, Arlington, VA 22217
1	ATTN: Code 471
	Commander, U.S. Air Force Wright Research & Development Center, Wright-Patterson Air Force Base, OH 45433-6523
1	ATTN: WRDC/MLLP, M. Forney, Jr.
1	WRDC/MLBC, Mr. Stanley Schulman
	U.S. Department of Commerce, National Institute of Standards and Technology, Gaithersburg, MD 20899
1	ATTN: Stephen M. Hsu, Chief, Ceramics Division, Institute for Materials Science and Engineering

No. of Copies	To
1	Committee on Marine Structures, Marine Board, National Research Council, 2101 Constitution Avenue, N.W., Washington, DC 20418
1	Materials Sciences Corporation, Suite 250, 500 Office Center Drive, Fort Washington, PA 19034
1	Charles Stark Draper Laboratory, 555 Technology Square, Cambridge, MA 02139
	Wyman-Gordon Company, Worcester, MA 01601
1	ATTN: Technical Library
	General Dynamics, Convair Aerospace Division, P.O. Box 748, Fort Worth, TX 76101
1	ATTN: Mfg. Engineering Technical Library
	Plastics Technical Evaluation Center, PLASTEC, ARDEC, Bldg. 355N, Picatinny Arsenal, NJ 07806-5000
1	ATTN: Harry Pebly
1	Department of the Army, Aerostructures Directorate, MS-266, U.S. Army Aviation R&T Activity - AVSCOM, Langley Research Center, Hampton, VA 23665-5225
1	NASA - Langley Research Center, Hampton, VA 23665-5225
	U.S. Army Vehicle Propulsion Directorate, NASA Lewis Research Center, 2100 Brookpark Road, Cleveland, OH 44135-3191
1	ATTN: AMSRL-VP
	Director, Defense Intelligence Agency, Washington, DC 20340-6053
1	ATTN: ODT-5A (Mr. Frank Jaeger)
	U.S. Army Communications and Electronics Command, Fort Monmouth, NJ 07703
1	ATTN: Technical Library
	U.S. Army Research Laboratory, Electronic Power Sources Directorate, Fort Monmouth, NJ 07703
1	ATTN: AMSRL-EP-M, W. C. Drach
1	AMSRL-EP-M, T. E. Koscica
1	AMSRL-EP-M, R. W. Babbit
	Director, U.S. Army Research Laboratory, Watertown, MA 02172-0001
2	ATTN: AMSRL-OP-CI-D, Technical Library
25	Authors